# A high order Newton method to solve vibration problem of composite structures considering fractional derivative Zener model

Mathias Ziapkoff, Laëtitia Duigou, Guillaume Robin, Jean-Marc Cadou, El Mostafa Daya

# A high order Newton method to solve vibration problem of composite structures considering fractional derivative Zener model

Mathias Ziapkoff[a], Laetitia Duigou[a], Guillaume Robin[b], Jean-Marc Cadou[a], and El Mostafa Daya[b]

[a]IRDL, UMR CNRS 6027, Univ. Bretagne Sud, Lorient, France
[b]LEM3, UMR CNRS 7239, Univ. de Lorraine, Metz, France

This paper presents a numerical method to solve the non-linear vibration problem of composite struc-tures made of many unidirectional fibers/matrix layers. To take into account damping properties of structures, fractional derivative Zener model for complex moduli is used in each layer. The frequency dependence of these models leads to a non-linear vibration problem. To solve it, a High Order Newton (HON) solver based on homotopy and perturbation techniques is proposed. Thus, the initial non-linear problem turns into a set of linear systems, easier to solve. Numerical results obtained by the HON solver are compared with experimental and numerical results of literature.

## 1. Introduction

Composite structures are used in a great deal of industrial fields where noise and vibration controls are sensitive issues. Indeed, noise dampening and the safety of people or equipments are concerns in industrial sectors, such as transportation, ship-builing, civil engineering, military engineering, etc. In order to decrease these vibrations, specific materials can be used. In this study, we focus on fiber reinforced composite structures and more precisely on their damped frequency and their structural damping. Many research-works deal with fiber reinforced composite damping. For the most part, they are experimental studies focusing on the influence of fiber rates, the orientation of the fibers or the matrix. Among these studies, frequency-dependence of damping has been highlighted [1–5]. This property is taken into account by considering complex frequency-dependent moduli. The material constitutive equation relating stresses and strains with respect to time or frequency and the linear viscoelasticity theory allow to express the complex frequency moduli variation both in frequency and time domains [6]. These complex and frequency-dependent moduli lead to frequency dependence of the stiffness matrix. Studying the vibrations of composite structures is therefore equal to solving a non-linear complex vibration problem. In order to analyze viscoelastically damped composite structures, the modal strain energy method [7, 8] or the direct frequency response method [8] define approximative values of complex mode. The QR-method [9] enables to solve complex problems but only in cases where the problems have few degrees of freedom or when moduli are constant complex. Three methods allow to solve any large scale complex eigenvalue problem. Chen et al. [10] propose a method coupling first order perturbation, an iterative algorithm and a reduced basis technique. The second method [11] is an Asymptotic Method based on homotopy [12, 13], perturbation technique [12, 14–16] and continuation procedure. In [17], Duigou et al. present a third method: high order iterative algorithms based on the coupling of homotopy transformation and of a perturbation technique. These three techniques have proved their effectiveness in the case of sandwich structures. However, none of them have been applied to fiber reinforced composite structures consisting of several layers with frequency-dependent behavior moduli. The study herein consists in adapting some of these techniques to fiber reinforced composite structural problems.

This paper aims to study the non-linear vibration problem of fiber reinforced composite structures made of many layers of unidirectional fibers. In order to take into account the frequency dependence, complex moduli of each layer are described here by the fractional derivative Zener model [6]. This model has four parameters. The frequency dependence of this model is introduced by an $\alpha$-power frequency term and leads to a non-linear vibration problem. In order to solve it, a High Order Newton (HON) solver based on homotopy and perturbation techniques is proposed in this paper. Initially put forward by Mallil et al. [13], this method has provided interesting results to solve the inherent vibrational problems of viscoelastic sandwich structures [11, 17]. The study herein aims to adapt these techniques to fiber reinforced composite structural problems and more specifically by flax-fibers. Structures with isotropic material or transversaly isotropic material may be considered.

The outline of the paper is the following. Firstly, the non-linear vibration problem to be solved is presented. Secondly, the proposed numerical method is described. Finally, the numerical results obtained are compared with experimental and numerical results in the literature, analyzed and used to validate the proposed method.

## 2. Governing equations

In this section, the problem equations are developed. Firstly, the modeling formulation of composite structures natural vibrations is obtained from the virtual work equation:

$$\int_V \left( S\delta E + \rho \frac{\partial^2 U}{\partial t^2} \delta U \right) dV = 0 \tag{1}$$

where $\rho$ denotes the density of the material. $S$, $E$ and $U$ are respectively the stress and strain tensors, and the generalized displacement at a point within the composite structure. Each of these terms can be expressed as harmonic time functions as follows:

$$U^* = ue^{j\omega^*}, \quad S^* = \sigma e^{j\omega^*}, \quad E^* = \varepsilon e^{j\omega^*} \tag{2}$$

with $j^2 = -1$ and $\omega^*$ is the complex frequency in damping presence.

The symbol "*" indicates a complex term in this paper. The stress-strain law allows to take the viscoelastic behavior of the composite structure into account:

$$\{\sigma^*\} = \mathfrak{C}^*(\omega^*)\{\varepsilon^*\} \tag{3}$$

where matrix $\mathfrak{C}^*(\omega^*)$ represents the viscoelastic constitutive law of the structure.

The combination of (1) and (3), and the use of the finite element discretization lead to the following free vibration problem of the composite structure:

$$\left[\mathbb{K}^*(\omega^*) - \omega^{*2}\mathbb{M}\right]\{U^*\} = \{0\} \tag{4}$$

$U^*$ denotes the complex nodal vibration eigenmode. $\mathbb{M}$ and $\mathbb{K}^*(\omega^*)$ are the constant real mass matrix and the frequency-dependent complex stiffness matrix respectively.

The free vibration problem of composite structures is complex non-linear. In the following section, a method to solve it is proposed.

## 3. Proposed method: High order Newton solver

In this section, we start by presenting a numerical method to solve the equation (4). We focus then on the global stiffness matrix $\mathbb{K}^*(\omega^*)$, depending on viscoelastic behavior laws considered in each layer of the composite structure. Finally, we develop the case of the fractional derivative Zener model.

### 3.1. High order Newton algorithm

In this paper, the viscoelastic behavior of each composite structure layer is represented by a frequency-dependent law. This leads to a composite structure whose stiffness matrix depends on the frequency in a complex way. Then, the problem of composite structure vibration is non-linear. In order to solve it, we propose to apply a High Order Newton (HON) method. Initially proposed by Mallil et al. [13], the HON method is based on homotopy and perturbation techniques. This principle of high order iterative algorithms has already been presented in the case of the following non-linear problems: vibrations of viscoelastic beams [17], geometrical and material defaults in beams [18] or a vibroacoustic interior problem [19]. As this principle has been effective in the cases mentioned above, we propose to apply this method to a composite structure vibration problem.

In order to simplify the resolution, the vibration problem (4) is rewritten as follows:

$$[\mathbb{K}^*(\omega^*) + \Omega^*\mathbb{M}]\{U^*\} = \{0\} \tag{5}$$

with $\Omega^* = -\omega^{*2}$. Then, solutions to the problem are sought in incremental form:

$$\begin{cases} U^* = U_0^* + \Delta U^* \\ \omega^* = \omega_0^* + \Delta\omega^* \\ \Omega^* = \Omega_0^* + \Delta\Omega^* \end{cases} \tag{6}$$

where $(U_0^*, \Omega_0^*)$ is a starting point which has to be chosen for the first iteration.

In the case of viscoelastic composite structures, layer's behavior laws are frequency-dependant. This leads to a stiffness matrix dependant on the frequency and that cannot be written simply as a function of $\omega^*$ (see Appendix A). Like the unknowns of non-linear vibration problem (5), the moduli and the stiffness matrix are searching in the following incremental form:

$$\begin{cases} \Lambda^*(\omega^*) = \Lambda^*(\omega_0^*) + \Delta\Lambda^* \\ \mathbb{K}^*(\omega^*) = \mathbb{K}^*(\omega_0^*) + \Delta\mathbb{K}^* \end{cases} \tag{7}$$

Using previous incremental forms (6) and (7), the main equation (5) of the problem is rewritten:

$$\begin{aligned} &\left[\mathbb{K}^*(\omega_0^*) + \Omega_0^*\mathbb{M}\right]\Delta U^* + \left[\mathbb{K}^*(\omega_0^*) + \Omega_0^*\mathbb{M}\right]U_0^* \\ &+ \left[\Delta\mathbb{K}^* + \Delta\Omega^*\mathbb{M}\right]U_0^* + \left[\Delta\mathbb{K}^* + \Delta\Omega^*\mathbb{M}\right]\Delta U^* = 0 \end{aligned} \tag{8}$$

We introduce a Linear operator $\mathbb{L}^*$ and the initial residual operator $R_0^*$ defined as follows:

$$\begin{cases} \mathbb{L}^* = \mathbb{K}^*(\omega_0^*) + \Omega_0^*\mathbb{M} \\ R_0^* = \mathbb{L}^* U_0^* \end{cases} \tag{9}$$

Therefore, the equation of the non-linear problem (8) is written as follows:

$$\begin{aligned} \mathbb{L}^*\Delta U^* + \Delta\Omega^*\mathbb{M}U_0^* = &-R_0^* - \Delta\mathbb{K}^* U_0^* - \Delta\mathbb{K}^*\Delta U^* \\ &- \Delta\Omega^*\mathbb{M}\Delta U^* \end{aligned} \tag{10}$$

At this step, we use the homotopy technique by adding an artificial parameter $\boldsymbol{\varepsilon}$ ranging from 0 to 1 such as for $\boldsymbol{\varepsilon} = 1$, we have the exact problem to solve:

$$\begin{aligned} \mathbb{L}^*\Delta U^* + \Delta\Omega^*\mathbb{M}U_0^* = &-\boldsymbol{\varepsilon}R_0^* - \boldsymbol{\varepsilon}\Delta\mathbb{K}^* U_0^* - \Delta\mathbb{K}^*\Delta U^* \\ &- \Delta\Omega^*\mathbb{M}\Delta U^* \end{aligned} \tag{11}$$

The unknowns are sought as truncated integro-power series. The perturbation parameter is the homotopy parameter $\boldsymbol{\varepsilon}$ :

$$\begin{cases} \Delta\mathbb{K}^*(\omega^*) = \sum_{i=1}^{N} \boldsymbol{\varepsilon}^i \mathbb{K}_i^* \\ \Delta\Omega^* = \sum_{i=1}^{N} \boldsymbol{\varepsilon}^i \Omega_i^* \\ \Delta\omega^* = \sum_{i=1}^{N} \boldsymbol{\varepsilon}^i \omega_i^* \\ \Delta U^* = \sum_{i=1}^{N} \boldsymbol{\varepsilon}^i U_i^* \end{cases} \tag{12}$$

Moreover, in order to keep a problem properly posed, the following orthogonality condition is added:

$$U^{*T}\mathbb{M}U_0^* = 0 \tag{13}$$

The latter choice is the same as in [17], and has already led to accurate results in studies about vibrations of viscoelastic shells. By inserting expansions (12) in (11) and adding the orthogonality condition (13), a set of linear problems coming from the identification of identical powers in $\boldsymbol{\varepsilon}$ is obtained:order 1:

$$\begin{cases} \mathbb{L}^* U_1^* + \boldsymbol{\Omega}_1^* \mathbb{M} U_0^* = -R_0^* \\ U_1^* \mathbb{M} U_0^* = 0 \end{cases} \tag{14}$$

order 2:

$$\begin{cases} \mathbb{L}^* U_2^* + \boldsymbol{\Omega}_2^* \mathbb{M} U_0^* = -\mathbb{K}_1^* U_0^* - \boldsymbol{\Omega}_1^* \mathbb{M} U_1^* - \mathbb{K}_1^* U_1^* \\ U_2^* \mathbb{M} U_0^* = 0 \end{cases} \tag{15}$$

order i > 2:

$$\begin{cases} \mathbb{L}^* U_i^* + \boldsymbol{\Omega}_i^* \mathbb{M} U_0^* = -\mathbb{K}_{i-1}^* U_0^* - \sum_{j=1}^{i-1} (\boldsymbol{\Omega}_j^* \mathbb{M} U_{i-j}^* + \mathbb{K}_j^* U_{i-j}^*) \\ U_i^* \mathbb{M} U_0^* = 0 \end{cases} \tag{16}$$

In the second member of (15) and (16), it appears terms $\mathbb{K}_{i-1}^*$ of the previous orders. Consequently, it is necessary to calculate them in order to solve each linear equation. The details of the computation are presented in Appendice (A) and the following subsections. Resolution of the systems (14, 15) and (16) allows to determine the unknowns $\mathfrak{X}_i^* = (U_i^*, \boldsymbol{\Omega}_i^*)^T$, and to deduce $\omega_i^*$ and $\mathbb{K}_i^*$ for each order i. Finally, all the previous linear problems can be rewritten in the following form:

$$\mathbb{L}_t(\mathfrak{X}_0^*)\mathfrak{X}_i^* = F_i \tag{17}$$

where $F_i$ stands for the right-hand side defined previously for each order *i*. The complex tangent operator which is the same for all the linear problems is given by:

$$\mathbb{L}_t^*(\mathfrak{X}_0^*) = \begin{bmatrix} \mathbb{L}^* & \mathbb{M}U_0^* \\ U_0^{*t}\mathbb{M} & 0 \end{bmatrix} \tag{18}$$

Resolution of the linear problems (17) is achieved by only one complex tangent operator triangulation and "*i*" foreward-backward substitution.

The final solution $\mathfrak{X}^*$ of the non-linear problem (with $\mathfrak{X}_i^* = U_i^*, \boldsymbol{\Omega}_i^*$) is achieved by setting $\boldsymbol{\varepsilon} = 1$ as follows:

$$\mathfrak{X}_{Poly}^*(\boldsymbol{\varepsilon} = 1) = \mathfrak{X}_0^* + \sum_{i=1}^{N} \boldsymbol{\varepsilon}^i \mathfrak{X}_i^* \tag{19}$$

Polynomial representation (19) can be replaced by Padé approximants in order to improve the convergence of the HON method. These Padé approximants are defined by the following expressions:

$$\mathfrak{X}_{Pade}^*(\boldsymbol{\varepsilon} = 1) = \mathfrak{X}_0^* + \sum_{i=1}^{(N-1)} \varepsilon^i f_i(\varepsilon) \mathfrak{X}_i^* \tag{20}$$

where $f_i(\varepsilon)$ are rational fractions having the same denominator as defined in [20].

In order to check the convergence, the relative residual $Res^{(p)}$ is estimated at each order (p) of the iteration:

$$Res^{(p)} = \frac{\left\| \left[ \mathbb{K}^{*(p)}(\omega^*) + \boldsymbol{\Omega}^{*(p)} \mathbb{M} \right] \left\{ U^{*(p)} \right\} \right\|}{\| \mathbb{K}(0) \left\{ U^{*(p)} \right\} \|} \tag{21}$$

Symbol $\| \bullet \|$ stands for the Euclidian norm of the vector $\bullet$ and $\mathbb{K}(0)$ for the elastic stiffness matrix. To determine residual, $U^{*(p)}$ and $\boldsymbol{\Omega}^{*(p)}$ are computed from series or Padé representation. $\mathbb{K}^{*(p)}(\omega^*)$ will be calculated directly by integrating the $\boldsymbol{\Omega}^*$ final form (19) or (20) in constitutive laws of stiffness matrix.

At each order, the residual with polynomial (19) or Padé (20) representation is determinded and stocked. At the end of iteration, a selection is made between polynomial (19) or Padé (20) representation at each order. The representation with the lowest relative residual (21) is selected, as it is considered as the "best order" among the N orders calculated [13]. The iterative procedure is stopped when the relative residual is lower than a given tolerance. If it is not the case, a new iteration is needed with an initial point corresponding to the solution of the previous iteration:

$$\mathfrak{X}_0^{*(p+1)} = \mathfrak{X}^{*(p)} \tag{22}$$

Then, a new operator $\mathbb{L}_t^*$ is computed and a new inversion matrix is necessary. It is to be noted that the tangent matrix is complex, which leads to a real matrix with a double size and so which induces a large computational cost.

When the convergence criterion is satisfied, damped pulsation $\Omega_d$ and structural damping $\eta_s$ are estimated from the real and imaginary parts of $\omega^*$. In this work, two definitions are used. The first one has been introduced in Duigou et al. [17] and defined by the following relations:

$$\begin{cases} \Omega_d = \sqrt{(\omega^r)^2 - (\omega^i)^2} \\ \eta_s = \dfrac{2\omega^r \omega^i}{(\omega^r)^2 - (\omega^i)^2} \end{cases} \tag{23}$$

The second one has been proposed by Litewka et al. [21] and Lewandowski et al. [22]:

$$\begin{cases} \Omega_d = \sqrt{(\omega^i)^2 + (\omega^r)^2} \\ \eta_s = \dfrac{\omega^i}{\Omega_d} \end{cases} \tag{24}$$

with:

$$\begin{cases} \omega^r = \dfrac{\sqrt{-\Omega^r + \sqrt{(\Omega^r)^2 + (\Omega^i)^2}}}{4} \\ \omega^i = \dfrac{-\Omega^i}{2\omega^r} \end{cases} \tag{25}$$

In the previous equations, symbols "r" and "i" represent real and imaginary part of complex number, such for example $\omega^*$ and $\boldsymbol{\Omega}^*$. Damped frequency is defined from damped pulsation by $f_d = \Omega_d/(2\pi)$.

This procedure is applied in an iterative way. The starting point of the first iteration is chosen as the solution

$(\Omega_{ud}, U_{ud})$ of the undamped problem associated to the damped problem (5), as defined in [17].

### 3.2. Fractional derivative Zener model

Composite structures are made of several layers and its behavior is introduced in expressions of moduli $\Lambda^* : E_L^*, E_T^*$ and $G_{LT}^*$ of each layer, with $L$ and $T$ being the longitudinal and the transversal axis of the considered layer. From the vibration tests of flax-fiber composite structures, it has been shown that they have a damping property [5, 23]. This property is a characteristic of viscoelastic materials [24, 25]: stress is a function of the strain history. That is why, here, we consider that each modulus $\Lambda^*$ is frequency-dependent: $E_L^*(\omega^*), E_T^*(\omega^*), G_{LT}^*(\omega^*)$.

In this paper, we consider the fractional derivative Zener model (Figure 1) for each layer and each orientation ($L$, $T$, $LT$). Fractional derivative Zener model has already been used to describe the viscoelastic behavior: [6, 21, 26]. Hafidi et al. [6] have investigated the characteristics of the fractional derivative Zener model of a flax-fiber reinforced composite structure with dynamic tests. Litewka and Lewandowski [21], have studied the dynamic characteristics of a viscoelastic plate by describing the plate material using the fractional derivative Zener model.

In the fractional derivative Zener model, the stress ($\sigma$)-strain ($\epsilon$) relation function of time (t) is defined in the following form:

$$\sigma(t) + \tau^\alpha D^\alpha[\sigma(t)] = \lambda_0\epsilon(t) + \lambda_\infty\tau^\alpha D^\alpha[\epsilon(t)] \tag{26}$$

where $\tau$ and $\alpha$ are respectively the relaxation time and the a real order fractional derivative coefficient ($0 < \alpha < 1$). $D^\alpha[\bullet]$ is an $\alpha$-order fractional derivative operator. The mechanical stiffnesses $\lambda_0$ and $\lambda_\infty$ are the dynamic moduli at very low frequency and at high frequency, respectively. Fourrier transformation allows us to write the equation (26) in the frequency domain, in the case of a steady state harmonic excitation, and thus obtain the following complex modulus:

$$\Lambda^*(\omega^*) = \frac{\lambda_0 + \lambda_\infty(j\omega^*\tau)^\alpha}{1 + (j\omega^*\tau)^\alpha} \tag{27}$$

In this model, the four real rheological parameters are $\lambda_0, \lambda_\infty$, $\tau$ and $\alpha$. In equation (27), the symbols $\lambda_0$ and $\lambda_\infty$ are the constant values of the rheological model and are defined by:

$$\begin{cases} \lambda_0 = (E_{L_0}, E_{T_0}, G_{LT_0}) \\ \lambda_\infty = (E_{L_\infty}, E_{T_\infty}, G_{LT_\infty}) \end{cases} \tag{28}$$

In order to solve the nonlinear vibration problem of composite structure, $\mathbb{K}_i^*$ terms must be determined. For this,

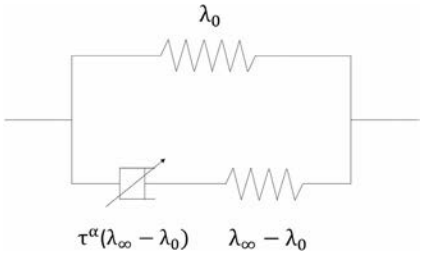


**Figure 1.** Fractional derivative Zener model.

moduli (7) are developped in series. The fractional derivative Zener model is complex non-linear and has in its expression a superscript parameter. So, the identification at each order of $\Lambda_i^*$ is not easy to carry out. To express these terms at each order, a new script is introduced. In order to express the real $\Lambda^r(\omega^*)$ and imaginary $\Lambda^i(\omega^*)$ parts of the moduli, we rewrite the terms $\omega^{*\alpha}$ and $j^\alpha$ in the following forms:

$$\begin{cases} (\omega^*)^\alpha = |\omega^*|^\alpha(\cos(\alpha\theta) + jsin(\alpha\theta)) \\ j^\alpha = \cos\left(\frac{\alpha\pi}{2}\right) + jsin\left(\frac{\alpha\pi}{2}\right) \\ \theta = arctan\left(\frac{\omega^i}{\omega^r}\right) \end{cases} \tag{29}$$

with $|\bullet|$ represents the modulus of the complex number $\bullet$. Then, by successive mathematical operations, the real and imaginary parts can be written as:

$$\begin{cases} \Lambda^r(\omega^*) = \lambda_0 \dfrac{(1 + (c_1+1)\omega_n^\alpha[\cos(\alpha\theta)c_2 - \sin(\alpha\theta)c_3] + c_1(\omega_n)^{2\alpha}}{1 + 2(\omega_n)^\alpha[\cos(\alpha\theta)c_2 - \sin(\alpha\theta)c_3] + (\omega_n)^{2\alpha}} \\ \Lambda^i(\omega^*) = \dfrac{\lambda_0(c_1-1)\omega_n^\alpha[\cos(\alpha\theta)c_3 + \sin(\alpha\theta)c_2]}{1 + 2(\omega_n)^\alpha[\cos(\alpha\theta)c_2 - \sin(\alpha\theta)c_3] + (\omega_n)^{2\alpha}} \end{cases} \tag{30}$$

with $\omega_n = \tau|\omega^*|$ and with the following constants:

$$c_1 = \frac{\lambda_\infty}{\lambda_0}, \quad c_2 = \cos\left(\frac{\alpha\pi}{2}\right), \quad c_3 = \sin\left(\frac{\alpha\pi}{2}\right) \tag{31}$$

With its $\alpha$-power term, fractional derivative Zener-type model is highly non-linear. So, the identification at each order of $\Lambda_i^r$ and $\Lambda_i^i$ are not easy to carry out. Indeed, terms in powers of $\alpha$ appear in their expressions. In order to develop unknowns in power series, equations have to be rewritten in quadratic forms [27]. As a consequence, new variables have to be introduced and their differential forms have to be used in order to rewrite the equation (30) in quadratic form. So as to present clearer expressions, frequency-dependency "$(\omega)$" of these terms is not included purposely. The following expressions will take the four rheological parameters: $\lambda_0$, $\lambda_\infty$, $\tau$, $\alpha$ into account. In order to introduce the polynomial approximations, the following expressions are defined:

$$\begin{cases} \nu^2 = (\omega_n^2 + \xi) \\ A = \nu^{2\alpha} \\ B = \nu^\alpha \\ X = \dfrac{\omega^i}{\omega^r} \\ \theta = arctanX \\ Z = X^2 \\ T = \cos(\alpha\theta) \\ S = \sin(\alpha\theta) \\ D = (c_1+1)[c_2T - c_3S] \\ F = 2[c_2T - c_3S] \\ H = (c_1-1)[c_3T + c_2S] \\ Y = FB \end{cases} \tag{32}$$

and their differential forms:

$$\begin{cases} vdA - 2\alpha A dv = 0 \\ vdB - \alpha B dv = 0 \\ d\theta = \dfrac{1}{1+Z} dX \\ dT = -\alpha S d\theta \\ dS = \alpha T d\theta \end{cases} \tag{33}$$

$\xi$ is a regularization parameter whose value is defined by the user. In numerical applications, this parameter varies between $\xi = 10^{-6}$ et $10^{-9}$. This regularization avoids numerical difficulties in the vicinity of a null pulsation. Symbol "$d$" designates the differential of the variable.

So, equations (30) become:

$$\begin{cases} \Lambda^r(\omega^*) = \lambda_0 \dfrac{1 + DB + c_1 A}{1 + Y + A} \\ \Lambda^i(\omega^*) = \lambda_0 \dfrac{HB}{1 + Y + A} \end{cases} \tag{34}$$

As $\omega^*$ is an unknown developed in series, variables $A$, $dA$, $B$, $dB$, $v$, $dv$, $D$, $F$, $H$, $\theta$, $T$, $S$, $X$, $Y$, $Z$ are sought in power series. Once the asymptotic developments of all variables in $\boldsymbol{\varepsilon}$ are introduced, the expressions of moduli and all variables at each order are obtained from the identification of the identical powers. Their expressions at order 0 and order 1 are given in Appendice B and at k-order, their expresssions are as follows:

Order k $\geq$ 2:

$$\begin{cases} \Lambda_k^r = \dfrac{\lambda_0 \left( B_0 D_k + B_k D_0 + \sum_{j=1}^{k-1} (B_j D_{k-j}) + c_1 A_k \right) - \Lambda_0^r (Y_k + A_k) - \sum_{j=1}^{k-1} \Lambda_j^r (Y_{k-j} + A_{k-j})}{1 + Y_0 + A_0} \\ \Lambda_k^i = \dfrac{\lambda_0 \left( B_0 H_k + B_k H_0 + \sum_{j=1}^{k-1} (B_j H_{k-j}) \right) - \Lambda_0^i (Y_k + A_k) - \sum_{j=1}^{k-1} \Lambda_j^i (Y_{k-j} + A_{k-j})}{1 + Y_0 + A_0} \end{cases} \tag{35}$$

with:

$$\begin{cases} v_k = \dfrac{2\omega_{n0}\omega_{nk} + \sum_{j=1}^{k-1} \omega_{nj}\omega_{nk-j} - \sum_{j=1}^{k-1} v_j v_{k-j}}{2v_0} \\ dv_{k-1} = k v_k \\ dA_{k-1} = \dfrac{2\alpha \left( A_0 dv_{k-1} + (\sum_{j=1}^{k-2} A_j dv_{k-j-1}) + A_{k-1} dv_0 \right) - v_{k-1} dA_0 - \sum_{j=1}^{k-2} v_j dA_{k-j-1}}{v_0} \\ dB_{k-1} = \dfrac{\alpha \left( B_0 dv_{k-1} + (\sum_{j=1}^{k-2} B_j dv_{k-j-1}) + B_{k-1} dv_0 \right) - v_{k-1} dB_0 - \sum_{j=1}^{k-2} v_j dB_{k-j-1}}{v_0} \\ A_k = \dfrac{dA_{k-1}}{k} \\ B_k = \dfrac{dB_{k-1}}{k} \\ X_k = \dfrac{\omega_k^i - X_0 \omega_k^r - \sum_{j=1}^{k-1} X_j \omega_{k-j}^r}{\omega_0^r} \\ \theta_k = \dfrac{kX_k - \sum_{j=1}^{k-1} j\theta_j Z_{k-j}}{k(1 + Z_0)} \\ Z_k = 2X_0 X_k + \sum_{j=1}^{k-1} X_j X_{k-j} \\ T_k = -\dfrac{\alpha}{k} \left[ kS_0\theta_k + \sum_{j=1}^{k-1} j\theta_j S_{k-j} \right] \\ S_k = \dfrac{\alpha}{k} \left[ kT_0\theta_k + \sum_{j=1}^{k-1} j\theta_j T_{k-j} \right] \\ D_k = (c_1 + 1)[c_2 T_k - c_3 S_k] \\ F_k = 2[c_2 T_k - c_3 S_k] \\ H_k = (c_1 - 1)[c_3 T_k + c_2 S_k] \\ Y_k = B_0 F_k + B_k F_0 + \sum_{j=1}^{k-1} B_j F_{k-j} \end{cases} \tag{36}$$

In this subsection, moduli are expressed at each order. However, it should be noted that moduli will not be estimated from the formula (7) at the end of an iteration. Indeed, each modulus ($E_L^*(\omega^*), E_T^*(\omega^*)$ and $G_{LT}^*(\omega^*)$) will be calculated by replacing $\omega^*$ by its final value.

The expressions of moduli at each order allow to define each stiffness matrix $\mathbb{K}_i^*$. Once the identification of the set of unknowns is achieved at all orders, the damped frequency and the structural damping of the non-linear problem of vibration of composite structures are determined by solving a linear problem sequence.

These moduli enable to define the global stiffness matrix $\mathbb{K}^*(\omega^*)$ in the following form, as demonstrated in Appendix A.

## 4. Numerical results

The present numerical procedure is applied to the vibration analysis of different composite structures. For each layer, we consider the Fractional derivative Zener model. The finite element method is used. The structures have been discretized using an eight-nodded quadrilateral $C^0$ isoparametric flat shell element with eight degrees of freedom per node. In order to describe the kinematics of the structure, the Third-Order Shear Deformation Theory (TSDT) is used [28, 29]. This theory is more accurate than the Classical Laminate plate Theory (CLT) and the First order Shear Deformation Theory (FSDT) as the TSDT theory takes the shear stress deformation into account. In order to validate the proposed High-Order Newton method, we propose to compare its results to examples from the literature [5, 6, 21]. In a first time, we consider an isotropic material plate with one layer. $E$ and $G$ follow Fractional derivative Zener model. In a second time, fiber-reinforced composite structures with several layers are studied. Each layer has three moduli $E_L$, $E_T$, $G_{LT}$ defined by Fractional derivative Zener model. In all cases, the tolerance for relative residual (21) is set to $10^{-8}$.

### 4.1. Validation of the HON method

The aim of this section is to apply the HON method to solve the non-linear vibration problem of one viscoelastic layer. We consider numerical tests presented by Litewka and Lewandowski [21]. We study a square plate ($0.5 \times 0.5 \times 0.05\, m^3$) simply supported on all four edges and made of an isotropic material. We mesh the plate with 100 elements, leading to 341 nodes. Poisson ratios $\nu$ and density $\rho$ are equal to 0, 45 and $1000\, kg/m^3$ respectively. The material follows the fractional derivative Zener-type viscoelastic law. The first damped pulsation and structural damping of the plate are considered. They are calculated with definitions (24). As in [21], damped frequency and damping of the plate will be studied according to the ratio of spring moduli in the fractional derivative Zener material $E_\infty/E_0$ and $G_\infty/G_0$. For the following three examples we represent them with the general expression $\lambda_\infty/\lambda_0$. In theses examples, the studied structure has different material properties.

#### 4.1.1. Example 1

In the first case, the plate is made from the viscoelastic material - Nitrile-Butadienne Rubber (NBR) described in [30].The full data used are defined in Table 1.

In [21], Litewka and Lewandowski have analyzed the plate under the influence of the ratio of spring moduli in the fractional derivative Zener material $E_\infty/E_0$ and $G_\infty/G_0$ taken from the range between 1 to 10. Here, we consider the ratio of $\lambda_\infty/\lambda_0$ equal to 10. We focus on the first mode of vibration according to their works. Figure 2 represents the number of needed iterations as a function of the truncation order in order to achieve convergence. The numbers of considered truncation order are $N=1$, which corresponds to the Newton algorithm, $N=5$, $N=15$, $N=20$ and $N=25$. The figure shows that the number of iterations needed to achieve the convergence criterion decreases when the truncation order increases. That is to say that the number of matrix inversion decreases. This figure highlights the benefit of a HON algorithm with high truncation order. That is a caracteristic of HON method.

Table 2 indicates the number of iterations to reach the damped pulsation and structure damping of [21] for several ratio $\lambda_\infty/\lambda_0$. A comparison is realized between Newton method and HON method with polynomial or Padé approximations. In this table, the number between parentheses indicates the truncation order of the last iteration. From $\lambda_\infty/\lambda_0 = 3$, we can see that HON method allows to decrease the number of iteration compared to a Newton method and so the number of matrix inversion. The interest of Padé approximants is shown for $\lambda_\infty/\lambda_0 = 10$. Indeed, Padé approximants enable to gain one iteration, so one matrix inversion.

In this example and the following ones, the $25^{th}$ truncation order does not reduce the number of iterations. So, we will consider truncation order equal to 20.

**Table 1.** Rheological parameters of fractional derivative Zener model for simply supported square plate of NBR isotropic material - Example 1.

| | $\lambda_0$ (MPa) | $\lambda_\infty$ (MPa) | $\tau(s)$ | $\alpha$ |
|---|---|---|---|---|
| E | 1,263 | 12,63 | 0,005 | 0,88 |
| G | 0,4355 | 4,355 | 0,005 | 0,88 |

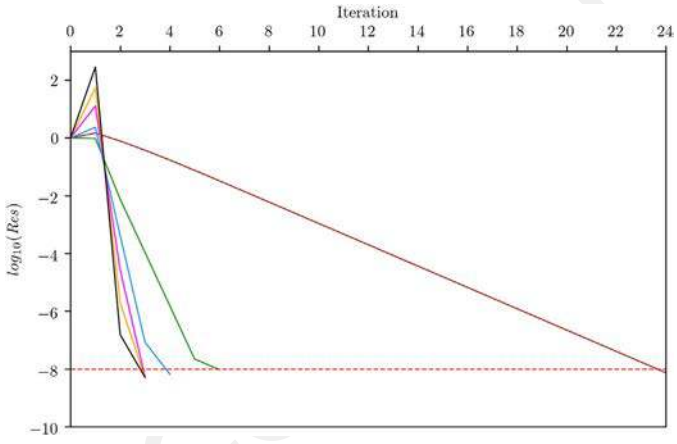


**Figure 2.** Simply supported square plate of NBR isotropic material - Example 1. Evolution of $log_{10}(Res)$ along the iterative process. Convergence is achieved when the convergence criterion is obtained (– – –). Five different scenarios presented: Newton (——), HON N = 5 (——), HON N = 10 (——), HON N = 15 (——),HON N = 20 (——), HON N = 25 (——).

#### 4.1.2. Example 2

In this example, the plate is made from the viscoelastic material - Paulstrane's Deltrane 350 rubber described in [31]. It follows the fractional derivative Zener-type viscoelastic law. The set of data used is given in Table 3.

Litewka and Lewandowski have analyzed the plate under the influence of the ratio of spring moduli in the fractional derivative Zener material $\lambda_\infty/\lambda_0$ taken from the range between 1 to 365. We focus on the first mode of vibration according to their works.

Figures 3 and 4 represent influence of ratio $\lambda_\infty/\lambda_0$ on damped pulsation and structural damping. These figures show good agreement between Litewka and Lewandowski's results [21] and HON method results. This example confirms that the calculation of the damped frequency and damping is correctly performed by the proposed method in the case of large ratio of $\lambda_\infty/\lambda_0$ for a little relaxation time, $\tau = 5,2 \times 10^{-7} s$. In the following example, a higher relaxation time is considered.

#### 4.1.3. Example 3

In this third example by Litewka and Lewandowski [21], the plate is made from the viscoelastic material - Nitrile-Butadienne Rubber - NBR- described in [30]. It follows the fractional derivative Zener-type viscoelastic law whose data set used is given in Table 4.

Litewka and Lewandowski have analyzed the plate under the influence of the ratio of spring moduli in the fractional derivative Zener material $\lambda_\infty/\lambda_0$ taken from the range between 1 and 10. We focus on the first mode of vibration according to their works. The relaxation time $\tau$ is $0,016\,s$, i. e. higher than in the previous examples. The problem to be solved is therefore more intricate.

**Table 2.** Example 1, considering different $\lambda_\infty/\lambda_0$. The damped pulsation and structure damping are computed using equations (24). Comparison between the number of iteration obtained with Newton Method (N = 1) and with HON solver with polynomial or Padé approximants for different truncation orders. The truncation order to achieve the required accuracy for the last iteration is given between parentheses.

| $\lambda_\infty/\lambda_0$ | Results | | N = 1 | N = 5 | | N = 10 | | N = 20 | | N = 25 | |
|---|---|---|---|---|---|---|---|---|---|---|---|
| | $\Omega_d$(rad/s) | $\eta_s$ | | Poly. | Padé | Poly. | Padé | Poly. | Padé | Poly. | Padé |
| 1 | 42,20 | 0 | 1 | 1 (1) | 1 (1) | 1 (1) | 1 (1) | 1 (1) | 1 (1) | 1 (1) | 1 (1) |
| 3 | 47,38 | 0,21 | 11 | 3 (1) | 3 (1) | 2 (2) | 2 (2) | 1(13) | 1 (12) | 1 (13) | 1 (12) |
| 5 | 56,11 | 0,40 | 17 | 4 (3) | 4 (3) | 2 (10) | 2 (10) | 2 (5) | 2 (5) | 2 (3) | 2 (3) |
| 7 | 70,37 | 0,52 | 22 | 5 (3) | 5 (3) | 3 (8) | 3 (6) | 2 (16) | 2 (14) | 2 (15) | 2 (13) |
| 10 | 95,95 | 0,55 | 24 | 6 (1) | 5 (5) | 4 (3) | 3 (9) | 3 (7) | 2 (19) | 3 (4) | 2 (19) |

**Table 3.** Rheological parameters of fractional derivative Zener model for simply supported square plate of Paulstrane's Deltrane 350 rubber.

| | $\lambda_0$ (MPa) | $\lambda_\infty$ (MPa) | $\tau(s)$ | $\alpha$ |
|---|---|---|---|---|
| E | 1 | 365 | $5{,}2 \times 10^{-7}$ | 0,59 |
| G | 0,35 | 127,75 | $5{,}2 \times 10^{-7}$ | 0,59 |

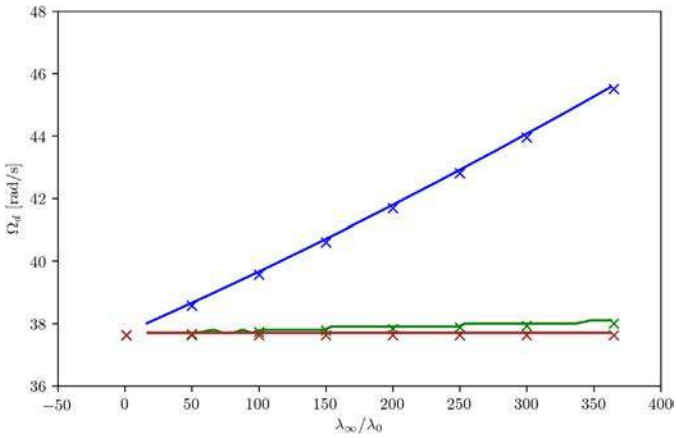


**Figure 3.** Simply supported square plate of Paulstrane's Deltrane 350 rubber - Example 2. Relation between first damped frequency and spring stiffness. Comparison between Litewka and Lewandowski [21] numerical results for $\alpha = 0,59$ (——), $\alpha = 0,80$ (——) and $\alpha = 1$ (——) and HON numerical results (respectively: ×, ×, ×).

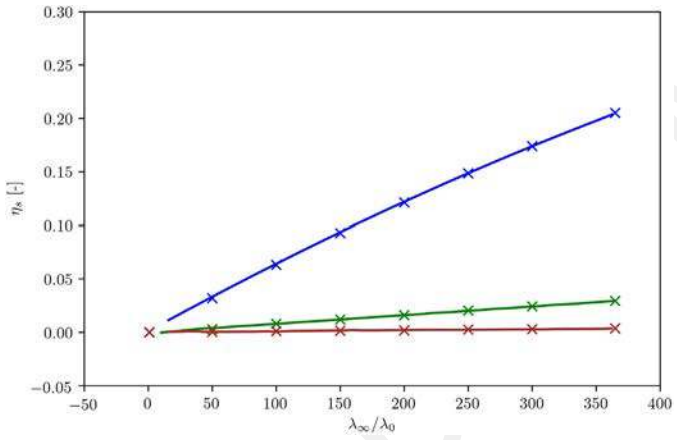


**Figure 4.** Simply supported square plate of Paulstrane's Deltrane 350 rubber - Example 2. Relation between structural damping and spring stiffness. Comparison between Litewka and Lewandowski [21]) numerical results for $\alpha = 0,59$ (——), $\alpha = 0,80$ (——) and $\alpha = 1$ (——) and HON numerical results (respectively: ×, ×, ×).

Figures 5 and 6 represent respectively the damped pulsation and the structural damping in function of the ratio $\lambda_\infty/\lambda_0$. On Figure 6, the HON method allows to find the Litewka results in the case of $\alpha = 0.95$, where the evolution of the damping is not linear. Thus, this method can solve high complex non linear problem. This example shows the robustess of HON method. It takes the influence of stiffness on the damping of the structure and the frequency-dependence of the damping into account.

By looking at the convergence of these solutions (Table 5), we can see once again, the interest of Padé approximants paired with a high order of truncation compared to the classical Newton method. Indeed, for example at $\alpha = 0,95$, HON solver associated with Padé approximants needs 2 iterations with truncation order egal to 10 whereas Newton

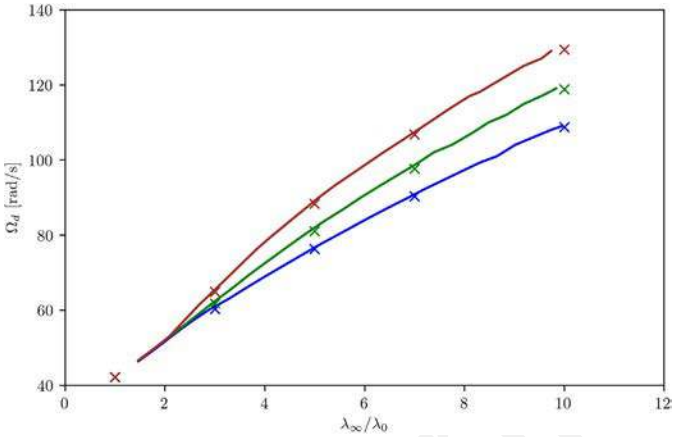


**Figure 5.** Simply supported square plate of NBR isotropic material - Example 3. Relation between first damped frequency and spring stiffness. Comparison between Litewka and Lewandowski [21] numerical results for $\alpha = 0,52$ (——), $\alpha = 0,76$ (——) and $\alpha = 0,95$ (——) and HON numerical results (respectively: ×,×,×).

**Table 4.** Rheological parameters of fractional derivative Zener model for simply supported square plate of NBR isotropic material - Example 3.

| | $\lambda_0$ (MPa) | $\lambda_\infty$ (MPa) | $\tau(s)$ | $\alpha$ |
|---|---|---|---|---|
| E | 1,263 | 12,63 | 0,016 | 0,52 |
| G | 0,4355 | 4,355 | 0,016 | 0,52 |

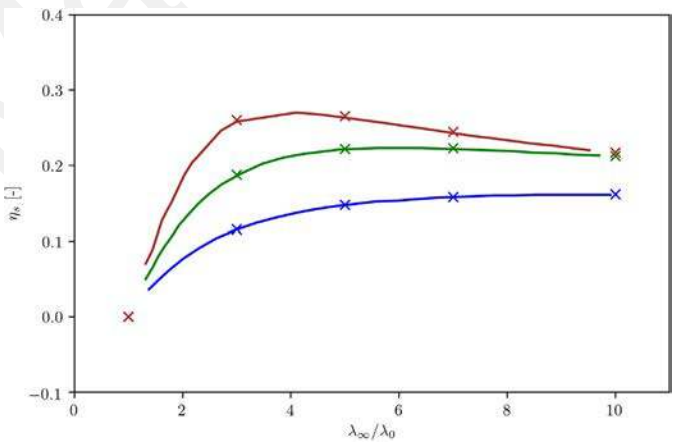


**Figure 6.** Simply supported square plate of NBR isotropic material - Example 3. Relation between strucural damping and spring stiffness. Comparison between Litewka and Lewandowski [21] numerical results for $\alpha = 0,52$ (——), $\alpha = 0,76$ (——) and $\alpha = 0,95$ (——) and HON numerical results (respectively: ×, ×, ×).

**Table 5.** Example 3 [21] considering $\lambda_\infty/\lambda_0$=10 and different values of $\alpha$. Comparison between the number of iteration obtained with Newton Method and with HON solver with Padé approximants. The number of orders for the last iteration is represented between brackets.

| $\alpha$ | Results | | Newton | HON + Padé |
|---|---|---|---|---|
| | $\Omega_d$ (rad/s) | $\eta_s$ | | |
| 0,52 | 108,73 | 0,16 | 10 | 2 (8) |
| 0,76 | 118,85 | 0,21 | 12 | 2 (10) |
| 0,95 | 129,34 | 0,22 | 14 | 2 (10) |

algorithm needs 14 iterations. In other words, HON method gains 12 iterations, so 12 matrix inversions. It leads to decrease of computational time.

With the help of these first three examples of isotropic material plates [21], we are able to validate the method by

Table 6. Rheological parameters of fractional derivative Zener model of a transversely isotropic material layer: flax-fibers/polymer.

| | $\lambda_0$ (GPa) | $\lambda_\infty$ (GPa) | $\tau$ (s) | $\alpha$ |
|---|---|---|---|---|
| $E_L$ | 19,2 | 20,70 | $2 \times 10^{-5}$ | 0,422 |
| $E_T$ | 5,03 | 5,63 | $2 \times 10^{-5}$ | 0,422 |
| $G_{LT}$ | 2,65 | 2,90 | $2 \times 10^{-5}$ | 0,422 |

Table 7. Free-fixed rectangular plate - transversely isotropic material. Comparison of iterations number between the HON solver (with or without Padé representation) and the classical Newton algorithm to compute the damped modes 1 to 7. Truncation order is indicated in brackets. Based on Hafidi et al. work [6].

| Bending mode | 1 | 2 | 3 | 4 | 5 | 6 | 7 |
|---|---|---|---|---|---|---|---|
| Newton | 3 | 3 | 3 | 3 | 3 | 3 | 3 |
| HON + Padé | 1(3) | 1(3) | 1(4) | 1(5) | 1(6) | 1(7) | 1(11) |

Table 8. Set of rheological parameters of fractional derivative Zener model obtained through an identification process based on the five bending mode given in Mahmoudi et al. [5].

| | $\lambda_0$ (GPa) | $\lambda_\infty$ (GPa) | $\tau$ (s) | $\alpha$ |
|---|---|---|---|---|
| $E_L$ | 25,28 | 29.66 | $5.2 \times 10^{-3}$ | 0,433 |
| $E_T$ | 2,265 | 2.90 | $5.2 \times 10^{-3}$ | 0,433 |
| $G_{LT}$ | 1,591 | 1,591 | $5.2 \times 10^{-3}$ | 0,433 |

considering a viscoelastic layer following the fractional derivative Zener model for different parameters, more or less complex. The association of the method with the Padé approximants in some cases proved again to be effective. In the following example, a composite structure is studied.

### 4.2. Application of the HON method for composite material applied to flax-fiber reinforced epoxy composite

We consider a free-fixed rectangular composite plate, presented by Hafidi et al. [6]. The flax-fiber reinforced epoxy composite plate ($V_f = 40\%$) has the following geometrical characteristics: $170 \times 10 \times 1\,mm^3$. It consists of 4 layers $[\pm 60^\circ]_s$. Each layer has the same material parameters. Poisson ratios $\nu_{LT}$, $\nu_{TL}$ and density $\rho$ are respectively equal to 0, 43, 0, 11 and $1289\,kg/m^3$. The viscoelastic law of fractional derivative Zener type has the parameters defined in Table 6. The mesh used has 10 elements, leading to 53 nodes.

The results in Figure 7 show the evolution of the structure damping (23) as a function of the vibration frequency for the $[\pm 60^\circ]_s$ laminate case and allow us to compare our numerical results with the experimental and numerical results by Hafidi et al. [6]. We only focus on the bending modes detected.

The points representing the numerical results obtained by the HON method follow the experimental and numerical curves obtained by Hafidi et al. [6]. This shows us that the calculation of the damped frequencies, necessary to calculate the structural dampings, is correctly performed by the proposed method. From the works by Hafidi et al. [6], bending modes 1 to 7 are studied. The iteration number between the classical Newton algorithm and the HON solver (with or without Padé representation, with best truncation order in brackets) are compared in Table 7. As these two methods give the same damped frequencies and damping, only the number of iterations is indicated. So, in the case of Free-fixed rectangular

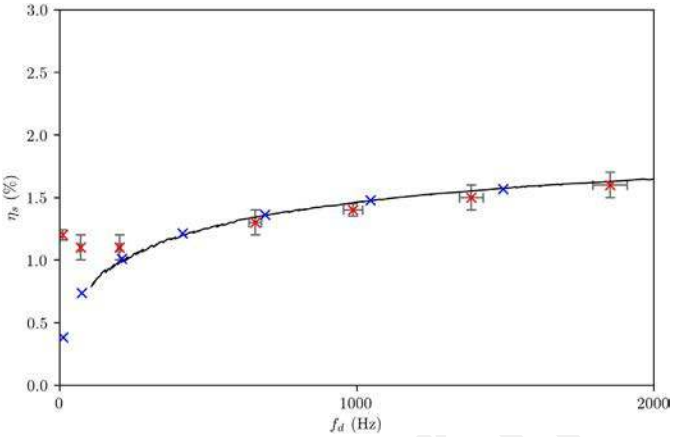


Figure 7. Free-fixed rectangular plate - transversely isotropic material. Frequency dependence of the structure damping for a $[\pm 60^\circ]_s$ laminated composite. Comparison between numerical (——) and experimental (×) results by Hafidi et al. [6] and HON numerical results (×).

flax-fiber reinforced epoxy composite plate, convergence is gained with one iteration when using the HON solver whereas the classical Newton algorithm needs three iterations that is to say three complex matrix inversions. We can note that the truncation order increases with the mode number. We apply Padé representation from the fifth order of truncation therefore, for the previous modes, Padé is not needed because convergence is obtained in the first four orders.

This example allows the HON method to be validated in the case of composite structures. HON enables to take into account several viscoelastic layers of different orientation and whose parameters follow the fractional derivative Zener model. In the following section, an identification of fractional derivative Zener model's parameters is performed from experimental results.

### 4.3. Application of the HON method for parameter identification of a flax-fiber composite structure

Now, we propose to study the example of Mahmoudi et al. [5]. We consider a free-fixed rectangular composite plate. The flax fiber reinforced epoxy composite plate ($V_f = 50\%$) has the following geometrical characteristics: $(250 \times 100 \times 3.1\,mm^3)$ for the plate made of 12 layers with $0^\circ/90^\circ$ as fiber directions and $(250 \times 100 \times 4.5\,mm^3)$ for the plate made of 16 layers oriented at $\pm 45^\circ$. 50 mm of the specimen length is clamped directly to the shaker. The structure is meshed with 10 elements leading to 53 nodes. The engineering constants of the composite are $E_L = 25,28\,GPa$, $E_T = 2,265\,GPa$, $G_{LT} = 1,591\,GPa$, $\nu_{LT} = 0,46$, $\rho = 1117\,kg/m^3$.

We focus on the bending mode detected experimentally by Mahmoudi et al. for two fiber orientations $0^\circ$ and $90^\circ$. We propose to test the proposed numerical method by taking into account one set of rheological parameters constructed from the engineering constants of the material. This set (Table 8) is obtained with an optimization algorithm. Five configurations corresponding to the first five experimental bending modes (two in the fiber orientation $0^\circ$ and three in the fiber orientation $90^\circ$) are used. To carry out the identification process, we use the well-known Nelder-Mead algorithm [32] for multidimensional

**Table 9.** Comparison of the damped frequencies $f_d$ (Hz) obtained experimentally and numerically by Mahmoudi et al. [5] and HON method with identified rheological parameters computed with expressions (23). Only the bending modes are analyzed.

| Mode | 0° | | | 90° | | |
|---|---|---|---|---|---|---|
| | Results from [5] | | Proposed method | Results from [5] | | Proposed method |
| | $f_{d(\text{exp.})}$ | $f_{d(\text{num.})}$ | $f_d$ | $f_{d(\text{exp.})}$ | $f_{d(\text{num.})}$ | $f_d$ |
| 1 | 58.8 | 59.8 | 62.821 | 18.2 | 17.2 | 18.943 |
| 2 | 377.9 | 371.1 | 395.33 | 119.4 | 111.9 | 121.72 |
| 3 | – | – | – | 304.0 | 313.2 | 344.40 |

**Table 10.** Comparison of the structural damping $\eta_s$ obtained experimentally and numerically by Mahmoudi et al. [5] and HON method with identified rheological parameters computed with expressions (23). Only the bending modes are analyzed.

| Mode | 0° | | | 90° | | |
|---|---|---|---|---|---|---|
| | Results from [5] | | Proposed method | Results from [5] | | Proposed method |
| | $\eta_{s(\text{exp.})}$ | $\eta_{s(num.)}$ | $\eta_s$ | $\eta_{s(\text{exp})}$ | $\eta_{s(num.)}$ | $\eta_s$ |
| 1 | 0,0295 | 0,0293 | 0.0271 | 0.0487 | 0,0484 | 0.0441 |
| 2 | 0,0172 | 0,0294 | 0.0192 | 0.0270 | 0,0484 | 0.0382 |
| 3 | – | – | – | 0,0401 | 0,0484 | 0.0306 |

unconstrained optimization without derivatives. The mesh used has 120 elements, leading to 405 nodes.

In this study, Mahmoudi et al. [5] investigate damped frequency and structural damping using an hysteretic model. We compare his results to the ones obtained with the proposed method (Tables 9 and 10).

These tables highlight the better accuracy of the identification process compared to hysteretic one. The proposed method respects the frequency-dependent damping behavior of the material observed experimentally. This aspect is not present in the numerical results of the previous model [5]. However, the objective is not achieved, a gap still exists between the numerical and experimental results. For greater accuracy, we need more bending modes leading to additional configurations for the optimization algorithm.

## 5. Conclusion

In this paper, a solver has been presented to study damped vibrations of fiber reinforced composite structures. These structures are made of many layers of unidirectional fibers and epoxy matrix. The damping is introduced considering a viscoelastic constitutive law for each layer. Here, viscoelasticy behavior is taken into account by fractional derivative Zener rheological model depending on angular frequency and temperature, so the problem to be solved is strongly non-linear. The proposed method, High Order Newton method, is based on homotopy and perturbation techniques, according to the method introduced by [13]. The HON solver can use Polynomial or Padé representation.

Several examples have been studied: isotropic material plate with different parameters of fractional derivative Zener rheological model, composite plates (different fractional derivative Zener rheological parameters for each modulus according to the directions (L, T, LT) and for each layer). Through these examples, HON solver has been valided by comparison with results from the literature or/and results obtained with the classical Newton algorithm, considered as the reference. The solver takes into account the frequency-dependance of the rheological model on structural damping. Also, its robustness has been proven. Indeed, the HON solver requires fewer iterations than the classical Newton method. Complexity of the fractional derivative Zener model renders convergence more intricate with the classical Newton method. It is to be noted that the same tangent operator is used at each order in the polynomial perturbation. Thus, the tangent operator is computed only once by iteration and kept for all the orders, contributing to reducing the number of iterations needed and the computational time. Moreover, the use of Padé representation greatly improves convergence. Finaly, we have considered the example of Mahmoudi et al. [5]. The HON solver validated and one set of parameters of fractional derivative Zener rheological model are tested in order to obtain experimental damped frequency and damping of the flax fiber reinforced epoxy composite plate. This last example highlighs the potential of such viscoelastic model compared to others such as an hysteretic one with an identification process. However, this kind of process needs a great number of configurations to give precise rheological parameters. That is why a serious experimental campaign will be organized in the future.

Therefore, the HON solver is able to solve the non-linear vibration problem of fiber-reinforced composite structures with fractional derivative Zener rheological model for each modulus (L, T, LT) in each layer. Hence, it will allow the identification of fractional derivative Zener law parameters associated with a consistent test campaign and/or an other identification algorithm such as Particle Swarm Optimization (PSO) [33, 34].


## Acknowledgment

The authors thank Christian Goualou for technical and theorical assistance in the identification part.


## Disclosure statement

No potential conflict of interest was reported by the authors.


## Funding

This work was supported by Agence Nationale de la Recherche. The authors wish to acknowledge the funding provided by the ANR AAPG2019 CE10 programme through the Bio-Damping project.

## References


[1] J. Berthelot, M. Assarar, Y. Sefrani, and A. El Mahi, Damping analysis of composite materials and structures, Compos. Struct., vol. 85, no. 3, pp. 189–204, 2008. DOI: 10.1016/j.compstruct.2007.10.024.

[2] R. Ni, D. Lin, and R. Adams, The dynamic properties of carbon-glass fibre sandwich-laminated composites: theoretical, experimental and economic considerations, Composites., vol. 15, no. 4, pp. 297–304, 1984. DOI: 10.1016/0010-4361(84)90710-9.

[3] A. Schultz and S. Tsai, Measurements of complex dynamic moduli for laminated fiber-reinforced composites, J. Compos. Mater., vol. 3, no. 3, pp. 434–443, 1969. DOI: 10.1177/002199836900300308.

[4] R. Crane and J. Gillespie, Characterization of the vibration damping loss factor of glass and graphite fiber composites, Compos. Sci. Technol., vol. 40, no. 4, pp. 355–375, 1991. DOI: 10.1016/0266-3538(91)90030-S.

[5] S. Mahmoudi, A. Kervoelen, G. Robin, L. Duigou, E. Daya, and J. Cadou, Experimental and numerical investigation of the damping of flax–epoxy composite plates, Compos. Struct., vol. 208, pp. 426–433, 2019. DOI: 10.1016/j.compstruct.2018.10.030.

[6] A. El-Hafidi, P. Gning, B. Piezel, M. Belaïd, and S. Fontaine, Determination of dynamic properties of flax fibres reinforced laminate using vibration measurements, Polymer Testing., vol. 57, pp. 219–225, 2017. DOI: 10.1016/j.polymertesting.2016.11.035.

[7] R. Rikards, A. Chate, and E. Barkanov, Finite element analysis of damping the vibrations of laminated composites, Comput. Struct., vol. 47, no. 6, pp. 1005–1015, 1993. DOI: 10.1016/0045-7949(93)90305-W.

[8] M. Soni, Finite element analysis of viscoelastically damped sandwich structures, Shock and Vibration Bull., vol. 55, no. 1, pp. 97–109, 1981.

[9] K. Bathe, Finite Element Procedures in Engineering Analysis, Prentice-Hall, NJ, 1982.

[10] X. Chen, H. Chen, and L. Hu, Damping prediction of sandwich structures by order-reduction-iteration approach, J. Sound Vibr., vol. 222, no. 5, pp. 803–812, 1999. DOI: 10.1006/jsvi.1998.2131.

[11] E. Daya and M. Potier-Ferry, A numerical method for nonlinear eigenvalue problems: application to vibrations of viscoelastic structures, Comput. Struct., vol. 79, no. 5, pp. 533–541, 2001. DOI: 10.1016/S0045-7949(00)00151-6.

[12] N. Damil, M. Potier-Ferry, A. Najah, R. Chari, and H. Lahmam, An iterative method based upon padé approximants, Commun. Numer. Meth. Engng., vol. 15, no. 10, pp. 701–708, 1999. DOI: 10.1002/(SICI)1099-0887(199910)15:10<701::AID-CNM283>3.0.CO;2-L.

[13] E. Mallil, H. Lahmam, N. Damil, and M. Potier-Ferry, An iterative process based on homotopy and perturbation techniques, Comput. Methods Appl. Mech. Engin., vol. 190, no. 13–14, pp. 1845–1858, 2000. DOI: 10.1016/S0045-7825(00)00198-5.

[14] A. Najah, B. Cochelin, N. Damil, and M. Potier-Ferry, A critical review of asymptotic numerical methods, Arch. Computat. Methods Eng., vol. 5, no. 1, pp. 31–50, 1998. DOI: 10.1007/BF02736748.

[15] M. Potier-Ferry, N. Damil, B. Braikat, J. Descamps, J.-M. Cadou, H. L. Cao and A.E. Hussein, Traitement des fortes non-linéarités par la méthode asymptotique numérique, Comptes Rendus de l'Académie des Sciences de Paris, Série II b., vol. 324, no. 3, pp. 171–177, 1997. DOI: 10.1016/S1251-8069(99)80022-0.

[16] J. Thompson and A. Walker, The non-linear perturbation analysis of discrete structure systems, Int. J. Solids Struct., vol. 4, no. 8, pp. 757–768, 1968. DOI: 10.1016/0020-7683(68)90054-1.

[17] L. Duigou, E. M. Daya, and M. Potier-Ferry, Iterative algorithms for non-linear eigenvalue problems. Application to vibrations of viscoelastic shells, Comput. Methods Appl. Mech. Engin., vol. 192, no. 11–12, pp. 1323–1335, 2003. DOI: 10.1016/S0045-7825(02)00641-2.

[18] G. Sliva, A. Brezillon, J. M. Cadou, and L. Duigou, A study of the eigenvalue sensitivity by homotopy and perturbation methods, J. Comput. Appl. Math., vol. 234, no. 7, pp. 2297–2302, 2010. DOI: 10.1016/j.cam.2009.08.086.

[19] B. Claude, L. Duigou, G. Girault, and J. M. Cadou, Study of damped vibrations of a vibroacoustic interior problem with viscoelastic sandwich structure using a High Order Newton solver, J. Sound Vibr., vol. 462, pp. 114947–114133, 2019. DOI: 10.1016/j.jsv.2019.114947.

[20] A. Elhage-Hussein, M. Potier-Ferry, and N. Damil, A numerical continuation method based on Padé approximants, Int. J. Solids Struct., vol. 37, no. 46–47, pp. 6981–7001, 2000. DOI: 10.1016/S0020-7683(99)00323-6.

[21] P. Litewka and R. Lewandowski, Dynamic characteristics of viscoelastic mindlin plates with influence of temperature, Comput. Struct., vol. 229, pp. 106181, 2020. DOI: 10.1016/j.compstruc.2019.106181.

[22] R. Lewandowski, P. Wielentejczyk, and P. Litewka, Dynamic characteristics of multi-layered, viscoelastic beams using the refined zig-zag theory, Compos. Struct., vol. 259, pp. 113212, 2021. DOI: 10.1016/j.compstruct.2020.113212.

[23] F. Duc, P. Bourban, C. Plumme, and J.-A. Månson, Damping of thermoset and thermoplastic flax fibre composites, Compos. Part A: Appl. Sci. Manufact., vol. 64, no. 2014, pp. 115–123, 2014. DOI: 10.1016/j.compositesa.2014.04.016.

[24] Ferry, J.D. (1980) Viscoelastic Properties of Polymers. 3rd Edition, John Wiley, New York.

[25] D. Roylance, Engineering Viscoelasticity, Massachusetts Insitute of Technology Cambridge, pp. 1–37, 2001.

[26] T. Pritz, Analysis of four-parameter fractional derivative model of real solid materials, J. Sound Vibr., vol. 195, no. 1, pp. 103–115, 1996. DOI: 10.1006/jsvi.1996.0406.

[27] B. Cochelin, N. Damil, and M. Potier-Ferry, Méthode Asymptotique Numérique, Hermès Science publications, Lavoisier, Paris, 2007.

[28] J. Reddy, Mechanics of laminated composite plates and shells: theory and analysis, CRC Press, USA 2003.

[29] J.-M. Berthelot, Matériaux Composites: Comportement Mécanique et Analyse des Structures, Editions Tec & doc, Lavoisier, France, 1999.

[30] L. Hongwei, G. Daniel, D. Shirley, and J.X. Zhaodong, Fractional differential equation bearing models for base-isolated buildings: framework development, J. Struct. Engin., vol. 146, no. 2, pp. 04019197, 2020.

[31] B. Morin, A. Legay, and J.-F. Deü, Reduced order models for dynamic behavior of elastomer damping devices, Finite Elements Anal. Design., vol. 143, no. 2018, pp. 66–75, 2018. DOI: 10.1016/j.finel.2018.02.001.

[32] J. Nelder, and R. Mead, A simplex method for function minimization, Computer J., vol. 7, no. 4, pp. 308–313, 1965. DOI: 10.1093/comjnl/7.4.308.

[33] J. Kennedy and R. Eberhart, Particle swarm optimization, IEEE International Conference on Neural Networks, 4, pp. 1942–1948, 1995.

[34] G. Bastos, L. Sales, N. Di Cesare, A. Tayeb, and J.-B. Le Cam, Inverse-pagerank-particle swarm optimisation for inverse identification of hyperelastic models: a feasibility study, J. Rubber Res., vol. 24, no. 3, pp. 447–460, 2021. DOI: 10.1007/s42464-021-00113-8.

[35] D. Gay, Matériaux Composites, Collection Matériaux, Hermès, 1997.

[36] A. Hallal, F. Fardoun, R. Younes, and F. Hage Chehade, Evaluation of longitudinal and transversal young's moduli for unidirectional composite material with long fibers, AMR., vol. 324, pp. 189–192, 2011. DOI: 10.4028/www.scientific.net/AMR.324.189.

[37] M. Matter, Identification modale numérique-expérimentale des propriétés élastiques et dissipatives de matériaux composites, Theses, Ecole Polytechnique Fédérale de Lausanne - LMAF, 2008. DOI: 10.5075/epfl-thesis-4215.

[38] M. Soula, T. Vinh, Y. Chevalier, T. Beda, and C. Esteoule, Measurements of isothermal complex moduli of viscoelastic materials over a large range of frequencies, J. Sound Vibr., vol. 205, no. 2, pp. 167–184, 1997. DOI: 10.1006/jsvi.1997.0978.

## Appendices: *A. Complex and frequency dependent stiffness matrix*

The composite structure is made up of a stack of UD composite layers. In order to have its complex constitutive relation, a layer is considered (Figure 8). In this study, the following hypotheses are applied: each layer has an transverse isotropic behavior ([35, 36], Poisson ratios are real and constant ([37, 38]) and longitudinal $E_L^*(\omega^*)$, transverse $E_T^*(\omega^*)$ and shear storage modulus $G_{LT}^*(\omega^*)$ all have the shape of fractional derivative Zener model (27), (30). Finally, we consider the plate theory in order to simplify the constitutive law to a $[5 \times 5]$ dimension matrix with $\sigma_{TT'}^*(\omega) = 0$. Therefore, in the local coordinates (L, T, T'), the constitutive law is written:

$$\left\{ \sigma^*(\omega) \right\}_{(L,T,T')} = \left[ C^*(\omega) \right] \left\{ \varepsilon^*(\omega) \right\}_{(L,T,T')} \tag{A.1}$$

either in a detailed manner:

$$\begin{Bmatrix} \sigma_{LL}^*(\omega) \\ \sigma_{TT}^*(\omega) \\ \tau_{TT'}^*(\omega) \\ \tau_{LT'}^*(\omega) \\ \tau_{LT}^*(\omega) \end{Bmatrix}_{(L,T,T')} = \begin{bmatrix} C_{11}^*(\omega) & C_{12}^*(\omega) & 0 & 0 & 0 \\ & C_{22}^*(\omega) & 0 & 0 & 0 \\ & & C_{44}^*(\omega) & 0 & 0 \\ & sym. & & C_{55}^*(\omega) = C_{66}^*(\omega) & 0 \\ & & & & C_{66}^*(\omega) \end{bmatrix} \times \begin{Bmatrix} \varepsilon_{LL}^*(\omega) \\ \varepsilon_{TT}^*(\omega) \\ \gamma_{TT'}^*(\omega) = 2\varepsilon_{TT'}^*(\omega) \\ \gamma_{LT'}^*(\omega) = 2\varepsilon_{LT'}^*(\omega) \\ \gamma_{LT}^*(\omega) = 2\varepsilon_{LT}^*(\omega) \end{Bmatrix}_{(L,T,T')} \tag{A.2}$$

with,

$$\begin{cases} C_{11}^*(\omega) = \beta E_L^*(\omega) \\ C_{22}^*(\omega) = \beta E_T^*(\omega) \\ C_{12}^*(\omega) = \beta \nu_{LT} E_T^*(\omega) \\ C_{44}^*(\omega) = G_{TT'}^*(\omega) = \dfrac{E_T^*(\omega)}{2(1+\nu_{TT'})} \\ C_{66}^*(\omega) = G_{LT}^*(\omega) \\ \beta = \dfrac{1}{1-\nu_{LT}\nu_{TL}} \\ \nu_{TL} = \nu_{LT} \dfrac{E_T^*(\omega)}{E_L^*(\omega)} \end{cases}$$

In order to study the composite structure vibration problem, the layer behavior law must be expressed in the structure frame, i.e. in the global frame (X, Y, Z):

$$\left\{ Q^*(\omega) \right\}_{(X,Y,Z)} = \left[ T(\gamma) \right] \left\{ C^*(\omega) \right\}_{(L,T,T')} \left[ T(\gamma) \right]^T \tag{A.3}$$

with $\left[ T(\gamma) \right]$, classical basis change matrix.

Once the expression of the layer behavior law is obtained in the frame of structure reference, the homogenization technique allows to determine the behavior law of the structure. In this paper, for all layers, moduli $E_L^*(\omega^*)$, $E_T^*(\omega^*)$ and $G_{LT}^*(\omega^*)$ have the shape of fractional derivative Zener model. This leads to a composite structure behavior law depending on frequency and using the variation Hamilton principle to a frequency-dependant stiffness matrix $\mathbb{K}^*(\omega^*)$.

## *B. Identification of moduli and variables in the case of fractional derivative Zener law*

order 0:

$$\begin{cases} \Lambda_0^r = \lambda_0 \dfrac{1 + B_0 D_0 + c_1 A_0}{1 + Y_0 + A_0} \\ \Lambda_0^i = \lambda_0 \dfrac{B_0 H_0}{1 + Y_0 + A_0} \end{cases} \tag{B.1}$$

with:

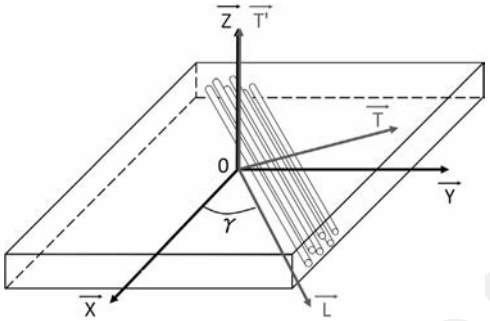


**Figure 8.** Representation of a layer.

$$\begin{cases} \nu_0 = \sqrt{\omega_{n0}^2 + \xi} \\ A_0 = \nu_0^{2\alpha} \\ B_0 = \nu_0^{\alpha} \\ X_0 = \dfrac{\omega_0^i}{\omega_0^r} \\ \theta_0 = arctan(X_0) \\ Z_0 = X_0^2 \\ T_0 = \cos(\alpha\theta_0) \\ S_0 = \sin(\alpha\theta_0) \\ D_0 = (c_1+1)[c_2 T_0 - c_3 S_0] \\ F_0 = 2[c_2 T_0 - c_3 S_0] \\ H_0 = (c_1-1)[c_3 T_0 + c_2 S_0] \\ Y_0 = B_0 F_0 \end{cases} \tag{B.2}$$

order 1:

$$\begin{cases} \Lambda_1^r = \dfrac{\lambda_0(B_0 D_1 + B_1 D_0 + c_1 A_1) - \Lambda_0^r(Y_1 + A_1)}{1 + Y_0 + A_0} \\ \Lambda_1^i = \dfrac{\lambda_0(B_0 H_1 + B_1 H_0) - \Lambda_0^i(Y_1 + A_1)}{1 + Y_0 + A_0} \end{cases} \tag{B.3}$$

with:

$$\begin{cases} \nu_1 = \dfrac{2\omega_{n0}\omega_{n1}}{2\nu_0} \\ d\nu_0 = \nu_1 \\ dA_0 = \dfrac{2\alpha A_0 d\nu_0}{\nu_0} \\ dB_0 = \dfrac{\alpha B_0 d\nu_0}{\nu_0} \\ A_1 = dA_0 \\ B_1 = dB_0 \\ X_1 = \dfrac{\omega_1^i - X_0\omega_1^r}{\omega_0^r} \\ \theta_1 = \dfrac{X_1}{1+Z_0} \\ Z_1 = 2X_0X_1 \\ T_1 = -\alpha S_0\theta_1 \\ S_1 = \alpha T_0\theta_1 \\ D_1 = (c_1+1)[c_2 T_1 - c_3 S_1] \\ F_1 = 2[c_2 T_1 - c_3 S_1] \\ H_1 = (c_1-1)[c_3 T_1 + c_2 S_1] \\ Y_1 = B_0 F_1 + B_1 F_0 \end{cases} \tag{B.4}$$